Korea-Australia Rheology Journal
Vol. 21, No. 3, September 2009 pp. 175-183

Numerical study of the effects of periodic body acceleration (PGZ) and bifurcation angle in the stenosed artery bifurcation

Kyoung Chul Ro and Hong Sun Ryou*
Department of Mechanical Engineering, Chung-Ang University, Seoul, Korea
(Received June 30, 2009; final version received July 30, 2009)

Abstract

This article describes the numerical investigation of blood flow in the stenosed artery bifurcation with acceleration of the human body. Using the commercial software FLUENT, three-dimensional analyses were performed for six simulation cases with different body accelerations and bifurcation angles. The blood flow was considered to be pulsation flow, and the blood was considered to be a non-Newtonian fluid based on the Carreau viscosity model. In order to consider periodic body acceleration, a modified, time-dependent, gravitational-force term was used in the momentum equation. As a result, flow variables, such as flow rate and wall shear stress, increase with body acceleration and decrease with bifurcation angle. High values of body acceleration generate back flow during the diastolic period, which increases flow fluctuation and the oscillatory shear index at the stenosis.

Keywords : periodic body acceleration, Computational Fluid Dynamics, stenosis, artery bifurcation, wall shear stress

1. Introduction

Blood flow characteristics in arteries can be altered by arterial disease, such as stenosis and surrounding circumstances. The altered blood flow and blood pressure may influence the development of disease and regional changes in blood rheology (Smedby, 1997). When patients with orthostatic hypotension move from the lying-down position to the standing position, their blood pressures can decrease instantaneously by as much as 20 mmHg (Bradley and Davis, 2003), so these people easily feel vertigo and have temporary visual and hearing problems due to the rapid movement and vibration of the body. Also, in the same situation, patients with hypertension may suffer from headache, a feeling of fatigue, an abnormal increase in pulse rate, and myocardial infraction (Zerwic, 1988).

Periodic acceleration (pGz) is forced from axial oscillating motion of whole body like a vibration. The human body often undergoes vibration and changes in gravitational forces in the daily activities of life, such as driving in vehicles, riding a roller coaster, and the rapid body movements that occur in sports activities. Although the human body is able to adapt to changes in the surroundings, a prolonged exposure of body to such vibrations leads to many health problems like headache, loss of vision, increase in pulse rate, abdominal pain, venous pooling of blood in the extremities and hemorrhage in the face, neck, eye sockets, lungs and brain (Hiatt *et al.*, 1961).

Adams *et al.* (2001, 2008) investigate the regional blood flow change during periodic body acceleration (pGz) with clinical trial of juvenile pigs. When 0.4 G pGz was subjected, regional capillary blood flows rate significantly increased in the outer layers of heart tissue (71%), cerebral tissue (183%), brain stem located lower part of brain (177%), and other of the vascular beds measured. Although pGz did not change arterial blood pressure or heart rate, the volume flow rate of blood pumped by the heart increased as the magnitude of pGz increased. Increased blood flow help revival of tissue by increase of oxygen delivery but prolonged and excessive periodic acceleration induce various side effects and heath problems as described above.

Burton *et al.* (1974) and Hooks *et al.* (1972) researched a clinical study of side effect by a change of blood flow when subjected extreme gravity and various periodic acceleration surroundings. The International Organization for Standardization (1997) has provided guidelines relating the magnitude of vibration to the degree of discomfort that passengers feel when using public transportation systems. According to ISO's guidelines, passengers feel uncomfortable if acceleration exceeds 0.3 m/s^2. Also, a guideline for whole body vibration for heavy equipment drivers was published by an EU research group (CEN Report 12349, 2006), which stated that there are risks to human health and safety when the human body is subjected to high levels

*Corresponding author: cfdmec@cau.ac.kr

of whole body vibration.

Due to physiological importance of body acceleration, many theoretical investigations have been carried out for the flow of blood under the influence of body acceleration with and without stenosis. Sud and Sekhon (1985) presented a mathematical model for flow in single arteries subject to pulsatile pressure gradient as well as the body acceleration. In their analytical treatment, blood has been assumed to be Newtonian fluid and flow as laminar, one-dimensional, and tube wall as rigid and uniformly circular. They define the periodic acceleration of axial direction (pGz) and pressure gradient during a pumping action of heart. The results shows that body acceleration does not affect the net flow of blood in arteries but affect the instantaneous value of flow variables such as flow rate, velocity and shear stress in the normal pumping actions. For body acceleration less than 0.01 G, the influence on blood flow in human arteries is negligible. However, when the body accelerations are more than about 0.5 G, the fluctuation of flow variables becomes relatively high. The results of their model have been used by Sud and Sekhon (1986) to further analyze the influence of body acceleration on arterial tree with 128 arteries. Their approach is based on other research on the blood flow under periodic acceleration.

Misra and Sahu (1988) developed a mathematical model to study the flow of blood through large arteries such as aorta and carotid arteries under the action of periodic body acceleration. Chaturani and Palanisamy (1991) studied the pulsatile flow of blood through rigid tube under the influence of body acceleration. The stenosis caused by intravascular plaques in the arterial system of humans or animals. This stenosis disturbs the normal pattern of blood flow within the artery.

Chakravarty and Mandal (1996) studied the effect of body acceleration on pulsatile flow through stenosed arteries. Chaturani *et al.* (1995) re-examined the study of Sud and Sekhon (1985) and obtained the analytical solution of flow variables using real variables. Recently, El-Shahed (2003) showed the effects of externally imposed periodic body acceleration on pulsatile flow of blood through a stenosed porous artery. All these studies were performed to considering blood as a Newtonian fluid, but in most cases, blood viscosity showed non-newtonian fluid from various number of experimental observations. Chaturani and Palanisamy (1990) have researched the effect of body acceleration on blood flow with blood as a Casson fluid. Mandal *et al.* (2007) used finite difference methods to develop a two-dimensional mathematical model for use in simulating stenosed arteries considering a moving wall effect with pre defined unsteady moving grid. Nagarani and Sarojamma (2008) investigated the effect of body acceleration on a mildly stenosed artery by modeling blood as a Casson fluid and Poiseuille flow using perturbation analysis assuming that the Womersley frequency parameter is small.

Table. 1 Simulation conditions for each cases

Cases	Percent stenosis	Magnitude of acceleration	Bifurcation angle	Frequency of acceleration and heat beat
Case 1	50%	0.0 m/s^2	26°	1.2 Hz
Case 2	50%	0.1 m/s^2	26°	1.2 Hz
Case 3	50%	0.5 m/s^2	26°	1.2 Hz
Case 4	50%	1.0 m/s^2	26°	1.2 Hz
Case 5	50%	0.0 m/s^2	15°	1.2 Hz
Case 5	50%	0.0 m/s^2	45°	1.2 Hz

All previous numerical research was performed in one-dimensional or two-dimensional analyses with an own developed mathematical model using the simplified governing equations and assumed boundary conditions. The mathematical model has merits of computing time and various applications but it is not well suited for the problems associated with complicated geometries, such as exist in asymmetric stenosed arteries. In order to perform complicated geometries and flow conditions, computational fluid dynamics (CFD) method is more appropriate.

2. Numerical details

In order to simulate the blood flow characteristics for various amplitudes of body acceleration and bifurcation angles of the idealized carotid artery with stenosis, three dimensional analyses were performed for six cases and each cases were listed in Table 1.

2.1. Modeling of a blood vessel

Fig. 1 shows a schematic view of the blood vessel, and it consists of three different bifurcation (α) angles (15, 26, and 45 degrees) with stenosis. Young (1968) model was used to model the radius of stenosis as:

$$R(y) = \left[r_0 - \frac{t_w}{2}[1 + \cos\pi((y-y_1)/y_0)] \right] \quad (1)$$

$$S_0 = (r_0 - R(y_1))/r_0 \times 100\% \quad (2)$$

where r_0 is the radius of the blood vessel without stenosis (4 mm), t_w is the maximum thickness of the stenosis ($r_0/2$), y_0 is the half length of the stenosis (8 mm), y_1 is the center position of the stenosis (80 mm), and S_0 is the percent reduction of the diameter due to the stenosis (50%).

2.2. Governing equations and boundary conditions

Numerical analysis was conducted for the blood flow, considering axial direction of periodic acceleration in the stenosed artery bifurcation. It was assumed that the flow

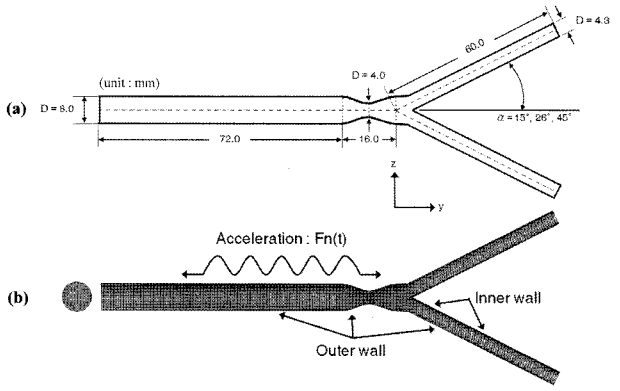

Fig. 1. Schematic representation and grid generation of artery bifurcation for the hemodynamic quantitative analyses. (a) The stenosed bifurcation artery has three bifurcation angles and stenosis rate of 50%. (b) hexagonal and O-grid shape mesh were used for the CFD simulation and we define two side of wall for the comparison of wall shear stress and oscillatory shear index. The periodic acceleration (pGz) is applied longitudinal axial of vessel.

through a blood vessel is laminar, incompressible, and unsteady. The blood was assumed to be a non-Newtonian fluid by the Carreau Viscosity Model (Cho *et al.*, 1985). Because young's modulus of stenosed artery wall is more higher than healthy artery wall (Tang *et al.*, 2004), the blood vessel wall was considered to be a rigid wall and a no-slip condition was applied to the wall. In order to simulate a bifurcated blood vessel, we performed a three-dimensional flow analysis.

The governing equations include the continuity equation and the momentum conservation equation, as follows:

$$\frac{\partial \rho}{\partial t} + \nabla \cdot (\rho \vec{v}) = 0 \tag{3}$$

$$\frac{\partial}{\partial t}(\rho \vec{v}) + \nabla \cdot (\rho \vec{v}\vec{v}) = -\nabla p + \nabla(\bar{\bar{\tau}}) + G(t) \tag{4}$$

where ρ is the fluid density, $\vec{v}$ is the vector of fluid velocity, p is the fluid pressure, t is time, and $\bar{\bar{\tau}}$ is the shear stress tensor. The term $G(t)$ is the momentum source of periodic acceleration, and it is needed for the momentum equation in the axial direction (y-direction).

The constitutive equations for non-Newtonian flow are required for blood rheology characteristics, and they are described by the second invariant of the shear rate tensor.

$$\bar{\bar{\tau}} = \eta \dot{\gamma} \tag{5}$$

where η is the apparent viscosity of the non-Newtonian fluid. The term $\dot{\gamma}$ indicates the shear rate, represented as follows:

$$\dot{\gamma} = \sqrt{\frac{1}{2}\sum_i \sum_j \dot{\gamma}_{ij}\dot{\gamma}_{ji}} \tag{6}$$

The cross, power, and Carreau models are the representative constitutive equations of non-Newtonian fluid viscosity. In this study, the Carreau Viscosity Model was used because it is suitable for representation of blood rheology characteristics:

$$\eta = \eta_\infty + (\eta_0 - \eta_\infty)[1 + (\lambda\dot{\gamma})^2]^{\frac{(n-1)}{2}} \tag{7}$$

where η_0 is the zero shear viscosity (0.056 Pa s), η_∞ is the infinite shear viscosity (0.00345 Pa s), λ is the time constant (3.313 s), and n is the power law index (0.356).

Periodic body acceleration was represented using sinusoidal functions that are composed of the frequency and the amplitude of acceleration pulsation. (Sud and Sekhon, 1985):

$$G(t) = a_0 cos(\omega_p t) \tag{8}$$

where α_0 is an amplitude of acceleration (0, 0.1, 0.5, or 1.0 m/s^2), ω_b is the frequency of periodic acceleration ($2\pi f_p$, f_p=1.2 Hz). From the relationship between frequency of heartbeat and the frequency of periodic acceleration (Sud and Sekhon, 1985), we assumed that the periodic acceleration and heart pressure have the same frequency.

For the pulsatile flow of blood, a pressure difference at the inlet and outlet boundaries was applied as a sinusoidal pressure pulse (Arntzenius *et al.*, 1970).

$$P(t) = (A_0 + A_1 cos(\omega_p t)), \tag{9}$$

where A_0 is the steady-state part of the pressure (1000 Pa), A_1 is the amplitude of its oscillatory component (200 Pa), and ω_p is the frequency of heart pulsation.

Pressure pulse had the same frequency as the periodic acceleration ($2\pi f_p$, f_p=1.2 Hz), and the outlet boundary condition was applied as a steady-state pressure boundary condition (Sud and Sekhon, 1985). The profiles of acceleration and pressure are shown in Fig. 2.

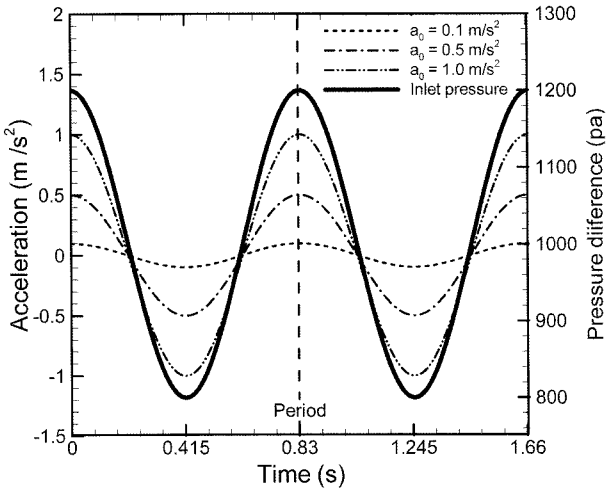

Fig. 2. Transient profiles of the periodic body acceleration and the pressure difference: Left axis is acceleration and right axis is pressure difference.

2.3. Computational Fluid Dynamics

Numerical simulations were performed with FLUENT V6.3, using the User-Defined Function (UDF) for the viscosity model, pressure, and acceleration profiles. The commercial CFD software FLUENT is based on the finite volume method. In this study, the second order scheme was used for the discretization of the governing equation. In this approach, higher-order accuracy was achieved at cell faces through a Taylor series expansion of the cell-centered solution about the centroid of the cell. Convergence criteria for numerical results were residuals (10^{-3}) of mass and velocity for all cells, and integrated quantities, such as volumetric flow rate, inlet velocity, and pressure, were also examined.

Unsteady flow analysis was conducted considering the effect of acceleration and pressure pulsation with a time step of 2 milliseconds and 4 periods. The solution time for each case was about 12 h on a 4-node, parallel, 2.4-GHz Intel, quad-core system.

2.4. Grid generation

The computational grid consisted of hexahedral meshes for three-dimensional geometry, and the commercial grid-generation software, ICEM-CFD, was used. The O-grid method was used to improve the mesh quality along the radial direction, as shown in Fig. 1. Grid independence was achieved with several refinements of the grids. We chose a grid size of approximately 0.5 mm with 189,000 cells (30 $\times$210$\times$30) and used refined grids of 0.1 mm on the near wall.

3. Results and discussion

3.1. Code validation

In order to validate the proposed periodic acceleration results in this paper, numerical simulation was performed under the same conditions as in a study by Sud and Sekhon (1985). They developed a one-dimensional mathematical model using a Bessel function for the calculation of arterial flow with periodic acceleration and performed analyses for flow characteristics with five different arteries under various periodic accelerations.

The volumetric flow rate in the artery without stenosis was calculated by following equation (Sud and Sekhon, 1985).

$$Q=\frac{\pi R^4}{8\mu_f}A_0=\frac{\pi R^2}{\omega_b}a_0 sin(\omega_b t+\phi)+\frac{\pi R^2}{\rho\omega_b}A_1 sin\omega_b t-4\pi R^2\sum_{n=1}^{\infty}e^{-\kappa\lambda_n^2 t}$$

$$\times\frac{A_1\omega_p^2(\kappa^2\lambda_n^4+\omega_b^2)-a_0\rho\kappa\lambda_n^2(\omega_b sin\phi+\kappa\lambda_n^2 cos\phi)(\kappa^2\lambda_n^4+\omega_p^2)}{\rho\kappa\lambda_n^4(\kappa^2\lambda_n^4+\omega_p^2)(\kappa^2\lambda_n^4+\omega_b^2)}$$

$$-\sqrt{2}\frac{\pi R}{\omega_b}a_0\sqrt{\frac{\mu_f}{\rho\omega_b}}[cos(\omega_b t+\phi)-sin(\omega_b t+\phi)]$$

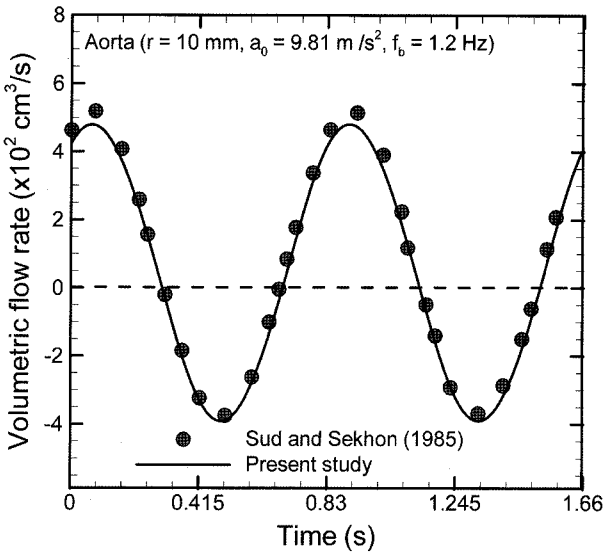

Fig. 3. Comparison of the volume flow rate in the aorta: μ= 0.004 Pa·s; R=10 mm; a_0=9.81 m/s^2; f_p=1.2 Hz; ϕ=0; A_1=73 Kgm^{-2}s^{-2}; A_0=14.6 Kgm^{-2}s^{-2}.

$$-\sqrt{2}\frac{\pi R}{\omega_p}A_1\sqrt{\frac{\mu_f}{\rho\omega_p}}(cos\,\omega_p t-sin\,\omega_b t) \quad (10)$$

where R is the radius of the artery, μ_f is the Newtonian viscosity of blood, ϕ is the phase angle of the periodic acceleration, κ is $\mu_f/\rho R^2$, and λ_n is the pole that were obtained from the zeros of the Bessel function.

Fig. 3 shows a comparison of volumetric blood flow rate in the aorta. The agreement between the results of mathematical and CFD simulation was very good. Errors of less than 8 percent and the validation test confirmed that the CFD method offered accurate and reliable solutions.

3.2. Detailed CFD simulations

3.2.1. The flow characteristics

The results of flow rate at the outlet of the artery are displayed in Fig. 4. The volumetric flow rate is shown as a periodic flow pattern after two periods because of the initial condition.

The flow rate changed in proportion to the amplitude of body acceleration due to the same frequency of heart pulse and periodic body acceleration. However, there was almost no change in the net flow rate over complete pulse cycles. Periodic body acceleration affected the instantaneous flow rate in the pulse cycle. Specifically, the instantaneous flow rate became a negative value when the amplitude of acceleration was 1.0 m/s^2, and a large backflow was observed at higher values of body acceleration during the diastolic period. These results agreed with the study of Arntzenius *et al.* (1970), El-Shahed (2003), Mandal *et al.* (2007), and Sud and Sekhon (1985).

In general, the pressure drop and flow resistance increased as the bifurcation angle increased for the same

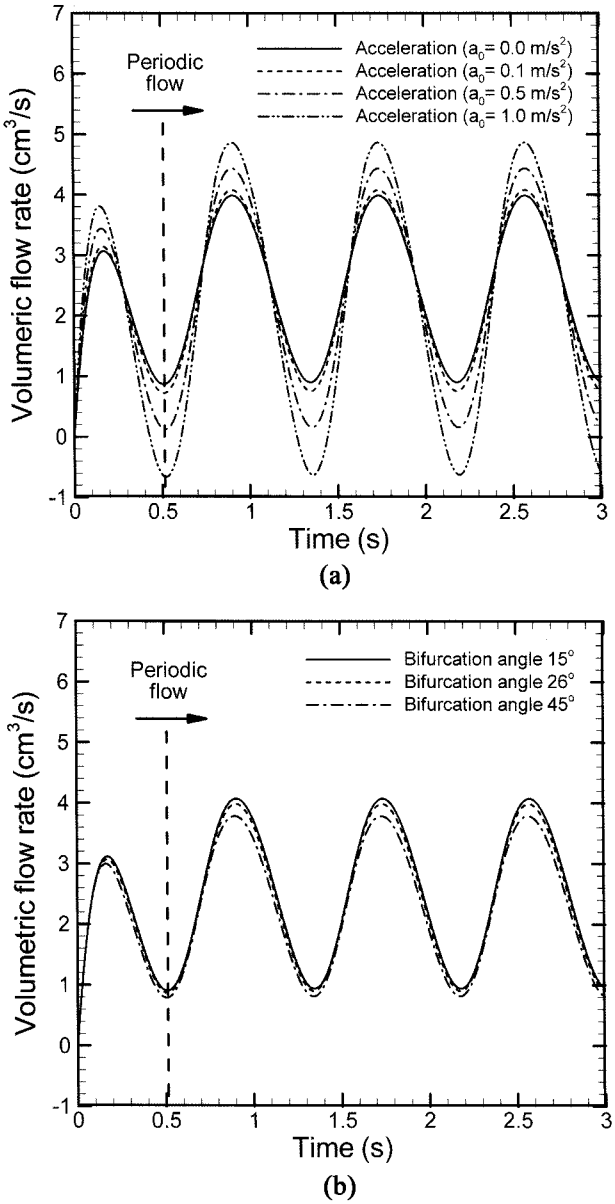

Fig. 4. Comparison of volume flow rate in the outlet. ((a) Effects of amplitude of periodic body accelerations in the 26 degree of bifurcation angle (b) Effects of bifurcation angles without the periodic body acceleration).

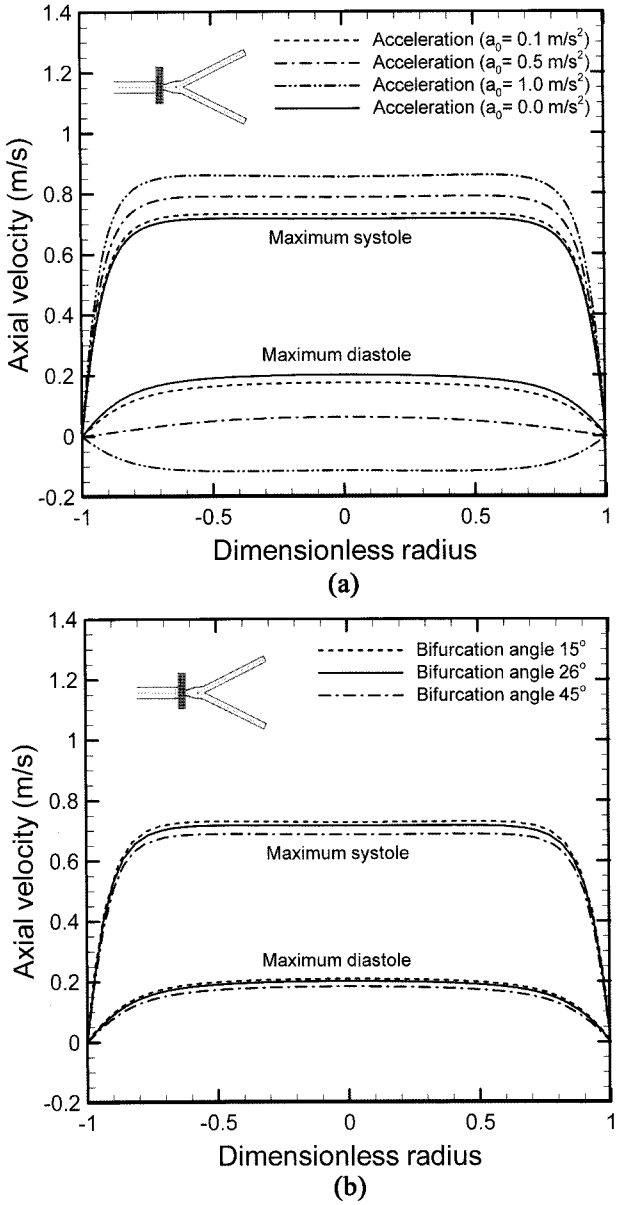

Fig. 5. Comparison of axial velocity in the middle of stenosis. ((a) Effects of amplitude of periodic body accelerations in the 26 degree of the bifurcation angle (b) Effects of bifurcation angles without the periodic body acceleration).

flow rate, but the same value of pressure difference was used at the inlet and outlet boundaries. So, the flow rate decreased as the bifurcation angle increased, and the differences in flow rate were reduced in the diastolic period when the flow rates were small.

Fig. 5 (a) illustrates an axial velocity profile along the diameter of a blood vessel at the center of stenosis. The shape of the axial velocity in the core region is not a parabolic curve due to the shear-thinning characteristics of the non-Newtonian fluid. It can be seen that the axial velocity distribution is similar to the results of flow rate shown in Fig. 4. Axial velocity increased as body acceleration increased during the systolic period, and back flow occurred with a body acceleration of 1.0 m/s^2 (0.1 G) during the diastolic period. Considering infinite shear viscosity, the Reynolds number ranged between 1,700 and 2,100. Under normal conditions, blood flow in most arteries is in the laminar regime, but it is possible that flow could become turbulent at higher values of body acceleration.

The axial velocity distributions at the center of the bifurcated artery are shown in Fig. 6.

The axial velocity near the inner wall was greater than it was near the outer wall. The peak velocity increased by about 22%, and the peak position was shifted closer to the

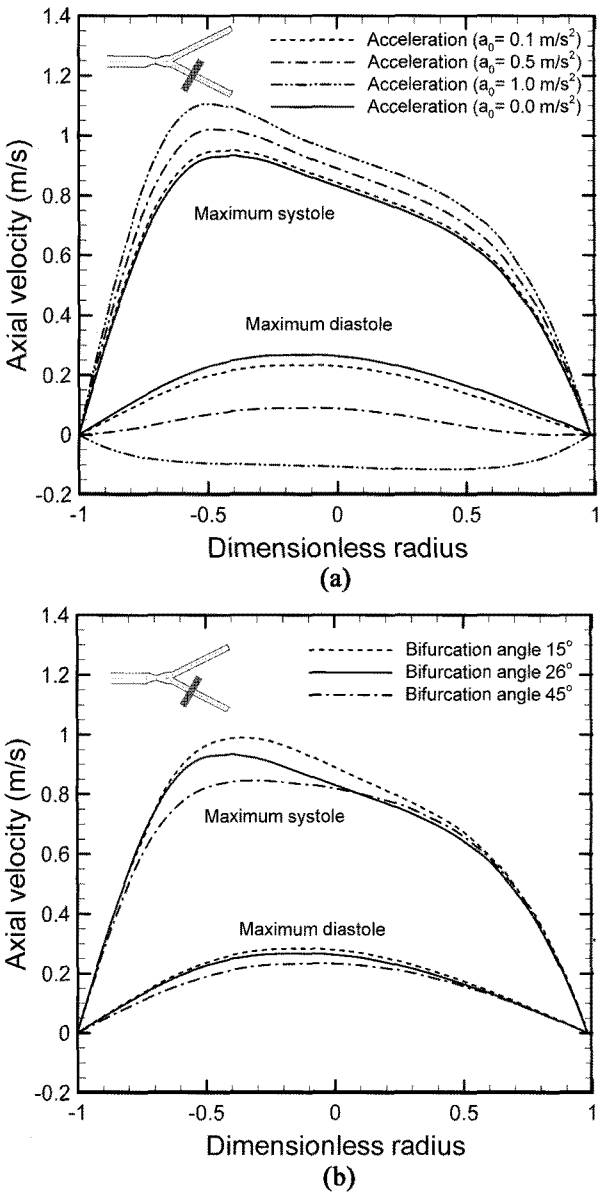

Fig. 6. Comparison of axial velocity in the middle of branched artery. ((a) Effects of amplitude of periodic body accelerations in the 26 degree of bifurcation angle. (b) Effects of bifurcation angles in the no periodic body acceleration)

near wall as body acceleration increased. On the contrary, axial velocity decreased as the bifurcation angle increased.

These results resulted from the fact that the inertia force of flow was higher than the centrifugal force caused by the geometrical shape, so the axial velocity at the inner wall was greater than the velocity at the outer wall. Therefore, a shift of axial velocity reduced during diastolic period and it did not occur at the peak diastole due to small flow rate and inertia force.

The significant flow recirculation is shown in Fig. 7 (a), (c), and (d). The flow recirculation occurred at the higher values of acceleration and at the lower angles of bifurcation, and it was highly related to the changes in wall shear stress and the oscillatory shear index (Ku *et al.*, 1985; He and Ku, 1996).

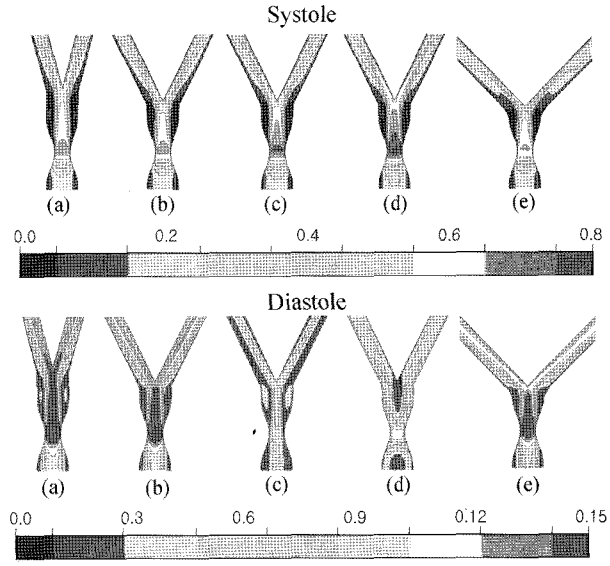

Fig. 7. Cross section velocity magnitudes of axial direction for each case: (1) 15 degree of bifurcation angle, and absence of periodic body acceleration; (b) 26 degree of bifurcation angle, and absence of periodic body acceleration; (c) 26 degree of bifurcation angle, and 0.5 m/s^2 of periodic body acceleration; (d) 26 degree of bifurcation angle, and 1.0 m/s^2 of periodic body acceleration; (e) 45 degree of bifurcation angle, and absence of periodic body acceleration. (unit : m/s).

3.2.2. The wall shear stress and oscillatory shear index

Wall shear stress (WSS) is related to the shear rate and the velocity gradient of the flow at the wall. Generally, the WSS of a healthy aorta is about 1~2 Pa, but a stenosed artery may have a WSS of more than 30 Pa (Fry, 1968).

The results on the WSS at the inner and outer wall are shown in Fig. 8, and the WSS contour is presented for each case in Fig. 9.

The uniform WSS is shown in the wall of the upper stream, and the two peak values of the WSS are indicated at the center of stenosis and at the apex of bifurcation. Downstream from the branched artery, the WSS values at the inner and outer walls are the same due to redeveloping flows. As shown in Fig. 8, a higher value of body acceleration increases the WSS in the systolic period. The bifurcation angle has small influence one WSS than magnitude of periodic acceleration relatively at the stenosis location, but the small bifurcation angle rapidly increases the WSS at the inner wall. These results were caused by the flow characteristics of bifurcation, mentioned above.

Fry (1969) and Caro *et al.* (1971) postulated that higher WSS values could damage the arterial wall. For this reason, endothelial disruption or denudation could lead to atherosclerosis. However, recently it has become widely accepted that low or oscillatory shear stress, rather than

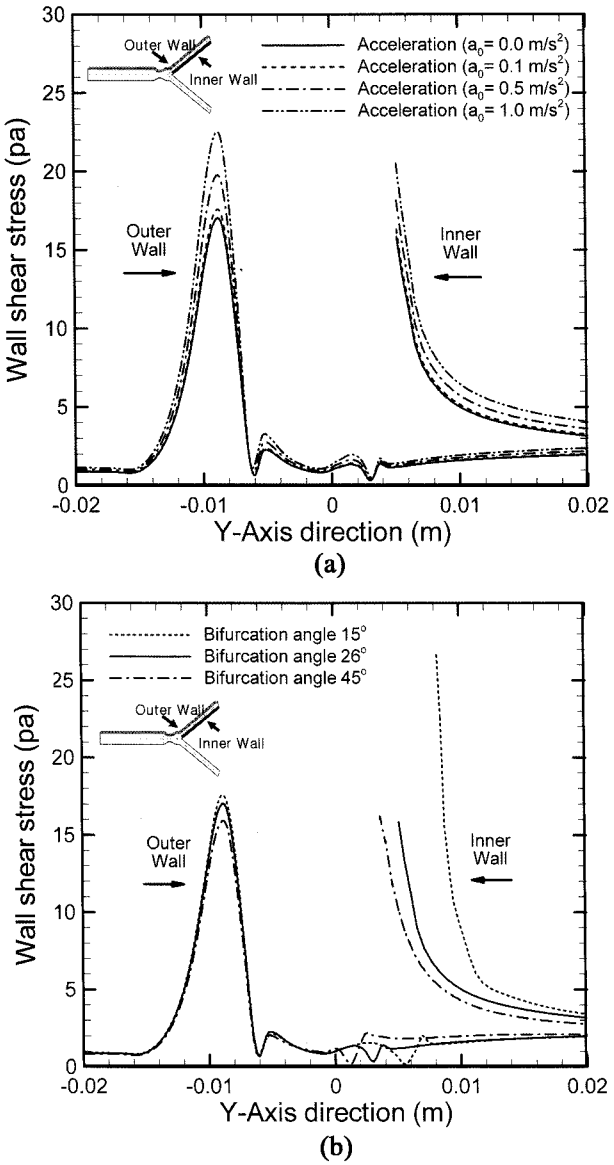

Fig. 8. Comparison of the wall shear stress (WSS) along the axial direction at the maximum systole. ((a) Effects of amplitude of periodic body accelerations in the 26 degree of the bifurcation angle (b) Effects of bifurcation angles without the periodic body acceleration).

high WSS values, contribute to atherosclerosis (Ku *et al.*, 1985; He and Ku, 1996).

The oscillatory shear index (OSI) defined by Ku *et al.* (1985) is an important parameter for the prediction of arterial disease. The OSI is defined by the following equation:

$$OSI = \frac{1}{2}\left(1 - \frac{\left|\int_o^T \vec{\tau}^{*} dt\right|}{\int_o^T \left|\vec{\tau}_w\right| dt}\right) \tag{11}$$

where $\vec{\tau}_w$ is the instantaneous WSS vector, and $\vec{\tau}^{*}$ is the WSS component acting in the direction opposite to the mean WSS vector. The OSI is a dimensionless value and

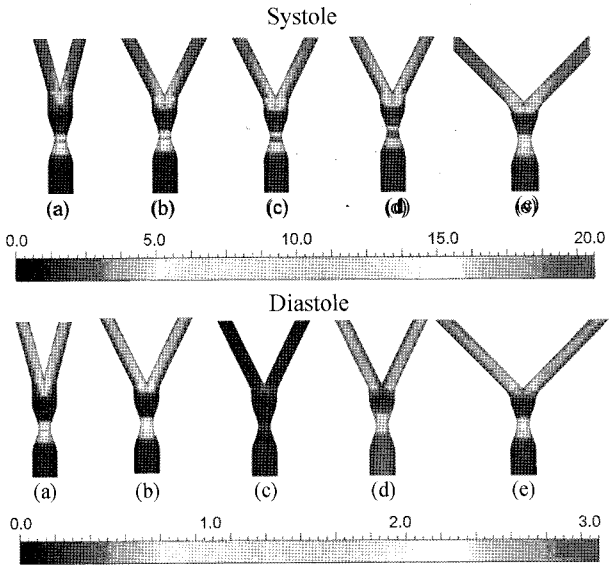

Fig. 9. Wall Shear Stress (WSS) contour for each case: (1) 15 degree of bifurcation angle, and absence of periodic body acceleration; (b) 26 degree of bifurcation angle, and absence of periodic body acceleration; (c) 26 degree of bifurcation angle, and 0.5 m/s^2 of periodic body acceleration; (d) 26 degree of bifurcation angle, and 1.0 m/s^2 of periodic body acceleration; (e) 45 degree of bifurcation angle, and absence of periodic body acceleration. (unit : Pa)

does not take account for the magnitude of the shear stress vectors. For purely oscillatory flow, the OSI reaches its maximum value of 0.5. As the shear stress acting in the opposite direction increases, the value of OSI increases, and the largest value of the OSI occurs in the flow separation and recirculation region.

Fig. 10 compares the OSI along the axial direction. Two peak values are shown at the same position as the WSS in all cases. It has been reported that atherosclerosis generally occurs at the branched artery due to the sudden change of section area and the curvature of the artery (Berger and Jou, 2000).

Figs. 8 and 10 indicate that body acceleration does not affect the health of the branched artery. However, in the stenosed artery, as body acceleration values increase, the value of the OSI and flow fluctuation increase. Thus, it seems that the higher value of body acceleration results in the increase of stenosis in the artery.

The OSI at the branched artery is affected by the bifurcation angle due to the variation of the WSS with time. The OSI is inversely proportional to the bifurcation angle, and the differences between the peak points are caused by changes in the distance between the origin and the apex of bifurcation due to geometrical differences.

4. Summary and conclusions

In this study, finite volume method (CFD) studies were

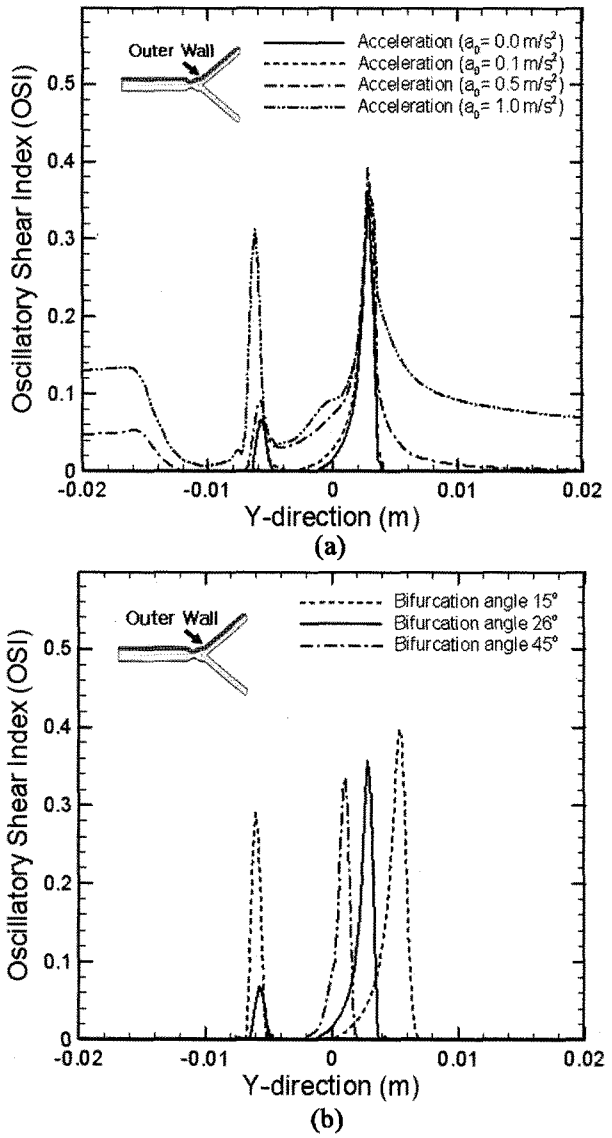

Fig. 10. Comparison of Oscillatory Shear Index (OSI) along the axial direction. ((a) Effects of amplitude of periodic body accelerations in the 26 degree of bifurcation angle (b) Effects of bifurcation angles without the periodic body acceleration)

performed for the idealized bifurcated blood vessel under periodic body accelerations. In order to validate the results, a numerical simulation was performed for the aorta model with a mathematical model developed by Sud and Sekhon (1985). The CFD results showed good agreement with the results obtained by the mathematical model.

In conclusion, in this study, periodic body acceleration affected instantaneous flow variables, such as flow rates, velocity distributions, and variations in the WSS. The amplitudes of fluctuation increased as imposed body acceleration increased. When the body acceleration was roughly greater than 0.6 m/s^2, back flow occurred during the diastolic period. However, the body acceleration did not influence blood flow in the branched artery.

As the bifurcation angle decreased, most flow variables increased due to small pressure drops in the flow field. The bifurcation angle affected the WSS at the inner wall and the OSI at the branched artery, but it had no effect in the region of stenosis.

From these results, we concluded that higher values of body acceleration have significant effects on blood flow in the stenosed artery. Therefore, we plan to research the various parameters of body accelerations and flow conditions in the stenosed artery bifurcation.

Acknowledgement

This work was supported by the Korea Research Foundation Grant funded by the Korean Government(MOE-HRD, Basic Research Promotion Fund)(KRF-2008-313-D00126)

References

Adams, J. A., J. A. Bassuk, J. Aris, H. Wu, V. Jorapur, G. A. Lamas and P. Kurlansky, 2008, Acute effects of "delayed post-conditioning" with periodic acceleration after asphyxia induced shock in pigs, *Pediatr. Res.* **64**, 533-537.

Adams, J. A., M. J. Mangino, J. Bassuk, P. Kurlansky and M. A. Sackner, 2001, Regional blood flow during periodic acceleration, *Crit. Care Med.* **29**, 1983-1988.

Arntzenius, A. C., J. Koops, F. A. Rodrigo, H. Elsbach and A. G. Brunmelen, 1969, Circulatory Effect of Body Acceleration given Synchronously with the Heartbeat (BASH), *Bibl Cardiol.* **26**, 180-187.

Berger, S. A. and L. D. Jou, 2000, Flows in Stenotic Vessels, *Annu Rev Fluid Mech.* **32**, 347-382.

Bradley, J. G. and K. A. Davis, 2003, Orthostatic Hypotension, *Am Fam Physician.* **68**, 2393-2398.

Burton, R. R., S. D. Leverett and S. D. Michaelson, 1974, Man at High Sustained +G Acceleration: A Review, *Aerosp Med.* **45**, 1115-1136.

Caro, C. G., J. M. Fitz-Gerald and R. C. Schroter, 1971, Atheroma and arterial wall shear: observation, correlation and proposal of a heart dependent mass transfer mechanism for atherogenesis, *Proc. R. Soc. Lond., B, Biol. Sci.* **177**, 109-159.

CEN Report 12349, 2006, Guide to good practice on Whole-Body Vibration. WBV Good practice Guide v6.7g, EUROPEAN COMMITTEE FOR STANDARDIZATION.

Chakravarty, S. and P. K. Mandal, 1996, A nonlinear two-dimensional model of blood flow in an overlapping arterial stenosis subjected to body acceleration, *Math Comput Model.* **24**, 43-58.

Chaturani, P. and V. Palanisamy, 1990, Casson fluid model for pulsatile flow of blood flow under periodic body acceleration, *Biorheology.* **27**, 619-630.

Chaturani, P. and V. Palanisamy, 1991, Pulsatile flow of blood with periodic body acceleration, *Int. J. Eng. Sci.* **29**, 113-121.

Chaturani, P., A. S. A. Isaac and Wassf, 1995, Blood flow with body acceleration forces, *Int. J. Eng. Sci.* **33**, 1807-1820.

Cho, Y.I., L. H. Back and D. W. Crawford, 1985, Experimental investigation of branch flow ratio, angel and Reynolds number effects on the pressure and flow fields in arterial branch models, *J Biomech Eng.* **107**, 257-267.

El-Shahed, M., 2003, Pulsatile flow of blood through a stenosed porous medium under periodic body acceleration, *Appl Math Comput.* **138**, 479-488.

Fry, D. L., 1968, acute vascular endothelium changes associated with increased blood velocity gradients, *Circ. Res.* **22**, 165-197.

Fry, D. L., 1969, certain histological and chemical responses of the vascular interface to acutely induced mechanical stress in the aorta of the dog, *Circ. Res.* **24**, 93-108.

He, X. and D. N. Ku, 1996, Pulsatile flow in the human left coronary artery bifurcation: average conditions, *J Biomech Eng.* **118**, 74-82.

Hiatt, E. P., J. P. Mecchan and Galambos, 1961, Reports on human acceleration, nasnrc washington dc, *publication* 901.

Hooks, L. E., R. M. Nerem and T. J. Benson, 1972, A momentum integral solution for pulsatile flow in a rigid tube with and without longitudinal vibration, *Int J Eng Sci.* **10**, 989-1007.

ISO, 1997, Mechanical vibration and shock - Evaluation of human exposure to whole-body vibration - Part 1: General requirements, International Organization for Standardization, 2631-1.

Ku, D. N., D. P. Giddens, C. K. Zarins and S. Glagov, 1985, Pulsatile flow and atherosclerosis in the human carotid bifurcation. Positive correlation between plaque location and low oscillating shear stress, *Arteriosclerosis.* **5**, 293-302.

Mandal, P. K., S. Chakravarthy, A. Mandal and N, Amin, 2007, Effect of body acceleration on unsteady pulsatile flow of non-Newtonian fluid through a stenosed artery, *Appl Math Comput.* **189**, 766-779.

Mirsa, J. C. and B. K. Sahu, 1988, Flow through blood vessels under the action of a periodic acceleration field : A mathematical analysis, *Comput Math Appl.* **16**, 993-1016.

Nagarani, P. and G. Sarojamma, 2008, Effect of body acceleration on pulsatile flow of Casson fluid through a mild stenosed artery, *Korea-Aust. Rheol. J.* **20**, 189-196.

Smedby, O., 1997, Do plaques grow upstream or downstream?: an angiographic study in the femoral artery, *Arterioscler Thromb Vasc Biol.* **17**, 912-918.

Sud, V. K. and G. S. Sekhon, 1985, Arterial flow under periodic body acceleration, *Bull. Math. Biol.* **47**, 35-52.

Sud, V. K. and G. S. Sekhon, 1986, Analysis of blood through a model of the human arterial system under periodic body acceleration, *J Biomech.* **19**, 929-941.

Tang, D., C. Yang, J. Zheng, P. K. Woodard, G. A. Sicard, J. E. Saffitz and C. Yuan, 2004, 3D MRI-Based multicomponent fsi models for atherosclerotic plaques, *Ann Biomed Eng.* **32**, 947-960.

Tang, D., C. Yang, S. Kobayashi, D. N. Ku, 2004, Effect of a lipid pool on stress/strain distributions in stenotic arteries: 3-D fluid-structure interactions (FSI) models, *J Biomech Eng.* **126**, 363-370.

Young, D. F., 1968, Effect of a time dependant stenosis on flow through a tube, *J Eng Ind Trans ASME.* **90**, 148-154

Zerwic, J. J., 1988, Symptoms of acute myocardial infarction: Expectations of a community sample, *Heart Lung.* **27**, 75-81.